Spectrochimica Acta Part A: Molecular and Biomolecular Spectroscopy 228 (2020) 117759

Contents lists available at ScienceDirect

Spectrochimica Acta Part A: Molecular and Biomolecular Spectroscopy

journal homepage: www.elsevier.com/locate/saa

# In situ detection of rice leaf cuticle responses to nitrogen supplies by depth-profiling Fourier transform photoacoustic spectroscopy

Gaoqiang Lv [a,b], Changwen Du [a,*], Fei Ma [a], Yazhen Shen [a], Jianmin Zhou [a]

[a] The State Key Laboratory of Soil and Sustainable Agriculture, Institute of Soil Science, Chinese Academy of Sciences, Nanjing 210008, China
[b] University of Chinese Academy Sciences, Beijing 100049, China

ARTICLE INFO

*Article history:*
Received 16 August 2019
Received in revised form 24 October 2019
Accepted 3 November 2019
Available online 6 November 2019

*Keywords:*
Plant cuticle
Nitrogen supply
FTIR-PAS
Depth-profiling
In situ detection

ABSTRACT

Plant cuticle is an important interface on the outmost region of plant and will make the response to environmental changes. However, research about how the variable nutritional status affect plant cuticle is limited. This was the first report about the manners of rice leaf cuticle in answer to different nutritional circumstances of nitrogen detected by the Fourier transform infrared photoacoustic spectroscopy (FTIR-PAS) which with a main superiority for in situ and depth-profiling in mid-infrared range. Rice leaves from the seedlings treated with three nitrogen levels designed as low (22N1), medium (N2) and high (N3) concentration were scanned by three moving mirror velocities (0.32 cm $s^{-1}$, 0.47 cm $s^{-1}$, and 0.63 cm $s^{-1}$) at 900–4000 $cm^{-1}$ to acquire the spectra of leaf surfaces. Well-resolved peaks had been detected at 3400, 2800, 1650, 1520 and 1050 $cm^{-1}$. Combining with the structures and compositions of cuticle, the spectra recorded with 0.63 cm $s^{-1}$ were identified to be from cuticle, and were used to analyze the responses of cuticle. Through curve-fitting, the absorption ratio of the peaks at ($cm^{-1}$) 1050/3400, 1050/2800 and 1650/2800 shown regular changes , which were suggested to corresponded with $\nu$(C—O)/$\nu$(O—H), $\nu$(C—O)/$\nu$(C—H) and $\nu$(C=C)/$\nu$(C—H) mainly. These ratios were supported to reflect the amount or variation of cuticle components, such as cutin, fatty alcohols, acids and unsaturated compounds. It provided insights about how nitrogen affected cuticles and showed great potentials to utilized FTIR-PAS for detecting cuticle variations.



## 1. Introduction

The epidermis of non-woody and aerial plant organs has a barrier named as cuticle covering the epidermal cell wall of the organs [1,2]. Plant cuticles are support to be composite structures and are composed of cutin, a covalently linked macromolecular scaffold; and waxes, a collectively termed for a variety of organic solvent-soluble lipids. Indeed, the structure of the cuticle can be divided into two domains based on their presumed chemical composition: cuticular layer, a cutin-rich domain with embedded polysaccharides; and cuticle proper, an overlying layer with a small amount of polysaccharide but enriched in waxes. The cutin is typically composed of the interesterified hydroxy fatty acids which with one or two additional midchain hydroxyl groups or an epoxy group. The waxes, include long-chain fatty acids, alcohols, aldehydes, esters and alkanes mainly, may deposit within the cutin matrix as intracuticular wax, or accumulate on its surface as epicuticular wax crystals, or films [3–8]. Mineral elements, for instance silicon, were also detected in *Ficus elastica* leaf cuticle with relatively high level [2]. Significant differences in cuticle composition can be observed depending on plant species, organs and even developmental stage of given organs [9,10].

As a hydrophobic interface between plant and environment, cuticle performs to protect plants against water loss and to defense against the abiotic and biotic stresses from environment [5,11]. Similarly, environmental conditions such as temperature, water availability, and light intensity can modify the amount and composition of the cuticle [7]. Moreover, the plants with a superhydrophilic cuticle have further biological advantages in terms of reduction of water content in the leaf surface, which is associated with the absorption of nutrients [12]. Iron deficiency, in addition, reduced the amount of soluble cuticular lipids in peach leaves, whereas it reduced the weight of the abaxial cuticle in pear leaves. And Fe-deficient leaves appeared less smooth than Fe-sufficient leaves [13]. However, the manner of cuticle makes response to nitrogen is still unknown.

Infrared (IR) spectroscopy is a non-destructive and accessible technique which has shown significant advantages in the chemical and structural analysis of plant cuticle. Nevertheless, traditional IR spectroscopy techniques present some drawbacks, such as the stringent specifications of sample preparation. Fourier transform infrared photoacoustic spectroscopy (FTIR-PAS) is a type of IR spectroscopy in the mid-infrared (MIR) region with practically no sample preparation, which makes it

* Corresponding author.
*E-mail address:* chwdu@issas.ac.cn (C. Du).

https://doi.org/10.1016/j.saa.2019.117759
1386-1425/

possible to perform in situ detection. And spectral in the MIR frequencies are often better resolved and more sensitive than in near infrared (NIR) domain. The capability to identify specific chemical groups has been the main role of Fourier transform MIR (FT-MIR) spectroscopy [8,14,15]. The analyte molecules absorb electromagnetic radiation, thereby causing local warming. Subsequently, thermal expansion generates pressure fluctuations, which can be detected by a sensitive microphone and transformed into spectral data [16–18]. The spectrum contains information about the sample and the detected signal is proportional to the sample concentration [19].

Based on its principle of recording spectrum, FTIR-PAS has unique advantage to carry out depth-profiling of the analyte through monitoring the modulation frequency by selecting various moving mirror velocities with different wavenumber regions [20,21]. The scanning depth of FTIR-PAS is positive correlation with the thermal diffusivity of the analyte and negative correlation with the product of wavenumber and moving mirror velocity (equals to modulation frequency). FTIR-PAS had been applied for depth-profiling about analyzing the spectral different of potato chips at different layers [22], detecting the pesticide residue layer on rice cuticle [23], and acquiring the spectra of *Cordyceps sinensis* in different depths for identifying the different sources of it [21]. It had showed a great potential for FTIR-PAS to carry out relevant studies of cuticle.

This study aimed to apply in situ and depth-profiling FTIR-PAS for detecting the responses of cuticle to plant nutrients. The spectra of rice leaves in the seedling stage were recorded by FTIR-PAS with three moving mirror velocities after the seedlings having been treated with low, medium, and high nitrogen concentrations. Results acquired by combining chemometrics and spectral information provided some insights into the patterns of cuticle in response to different nitrogen circumstances and into the utilization of FTIR-PAS for studying cuticles of plant as well.

## 2. Materials and methods

### 2.1. Plant material and growth conditions

Rice (*Oryza sativa* 'Nipponbare') seeds were surface sterilized in 0.5% (*v*/v) NaOCl for 15 min, rinsed and germinated on a plastic mesh with 0.5 mM $CaCl_2$ solution in a plastic container for 5 d. Then the seedlings were transferred into half strength nutrient solution which was provided by the International Rice Research Institute (IRRI) [24]. The IRRI nutrient solution contained 1.5 mM $NH_4NO_3$, 0.3 mM $NaH_2PO_4$, 0.5 mM $K_2SO_4$, 1.0 mM $CaCl_2$, 1.6 mM $MgSO_4$, 0.5 mM $NaSiO_3$, 20 μM Fe-EDTA, 0.075 μM $(NH_4)_6Mo_7O_{24}$, 18.9 μM $H_3BO_3$, 9.5 μM $MnCl_2$, 0.1 μM $CuSO_4$, 0.2 μM $ZnSO_4$, and 70.8 μM citric acid. Si was supplied as silicic acid. After germination, similar small seedlings with two leaves were transferred into 3-L plastic pots treated with modified nutrient solution. In the solution, only the nitrogen concentration was modified by adjusting the consumption of $NH_4NO_3$ and using three treatments of low nitrogen 1.5 mM (half of $NH_4NO_3$ concentration compared to IRRI nutrient solution), medium nitrogen 3.0 mM (normal level of $NH_4NO_3$ concentration compared to IRRI nutrient solution), and high nitrogen 6.0 mM (double of $NH_4NO_3$ concentration compared to IRRI nutrient solution), which were abbreviated as N1, N2, and N3, respectively. There were 10 seedlings in each container with 5 replicates. The pH was adjusted to 5.5 every day and the solution was renewed every 2 d. The plants were grown in a controlled-environment growth chamber under a 14-h/25 °C day with 2000 LX light intensity and a 10-h/20 °C night without light.

There were 5 leaf samples which were in the same growth status were taken at the seedling stage (25 d after treatment) from each nitrogen supply set, and the fourth leaf of each plant was selected for spectral determination. The leaves were cut to remove 5 cm of the tip and 10 cm of the petiole; thereafter, the leaves were punched into five equally spaced discs from the tip to the petiole (diameter 10 mm), named as P1, P2, P3, P4, and P5 (Fig. 1a). The front surfaces of the 25 leaf discs in total from each set were used for spectra recording.

### 2.2. Spectra recording

A Fourier transform infrared spectrometer (Nicolet 6700, Thermo Scientific, USA) equipped with a photoacoustic cell (model 300, MTEC, USA) was used to record photoacoustic spectra of all samples. The sample leaf discs were placed in a cell holding cup (diameter 10 mm, height 3 mm), which was purged with dry helium (10 mL $min^{-1}$) for 12 s to remove interferences from $CO_2$ and $H_2O$ (Fig. 1b). The scans were performed in the mid-infrared wave-number range of 900–4000 $cm^{-1}$ with a resolution of 4 $cm^{-1}$ and scanning times 64, using three moving mirror velocities of 0.32, 0.47, and 0.63 cm $s^{-1}$ for depth-profiling. There were 10 repetitions per leaf disc sample, which were used to obtain an average spectrum to represent the spectrum of the sample, and every obtained spectrum was normalized against a carbon black reference. Finally, there were 75 spectra in each nitrogen supply set were used for followed analyses.

### 2.3. Data processing

All obtained leaf spectra were filtered using the Savitzky-Golay function (25 points and first polynomial order filtering) and standardized by the software MATLAB 2016b (MathWorks Inc., USA). Ten replicates for each leaf disc sample were averaged by the mean function of MATLAB 2016b.

The dimensions of spectral data were reduced by principal component analysis (PCA) using the software MATLAB 2016b, and then plotted the distributions between the main principal components (PC) to identify the heterogeneity of the sample.

PeakFit 4.0 (AISN Software Inc., USA) was used for curve-fitting analysis and the filtering parameter of deconvolution was applied to isolate the target information hidden in the spectra. After peak fitting analysis, the photoacoustic signal intensity ratio of characteristic peaks was utilized to evaluate the content variation of the compounds in the cuticle.

The function was used to calculate the average profiling depths of specific absorption bands under different modulation frequencies

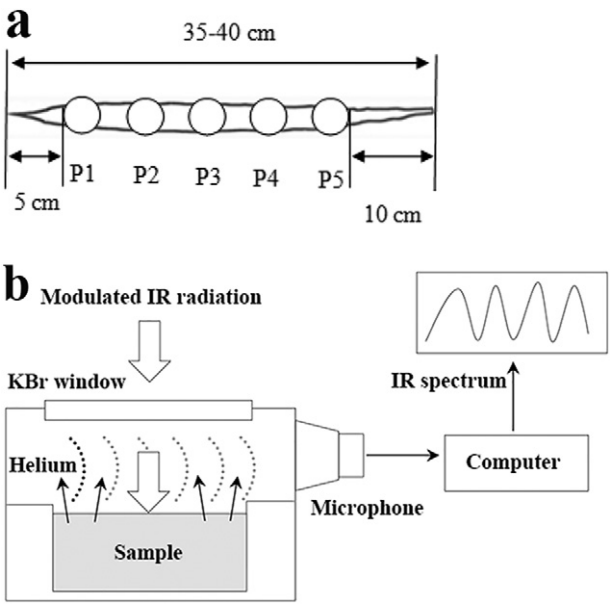


**Fig. 1.** The positions selected on the leaf samples. The seedling stage leaves were cut off with 5 cm of the tip and 10 cm of the petiole; thereafter, the leaves were punched into five equally spaced discs from tip to petiole, named as P1, P2, P3, P4, and P5 respectively (a). And the schematic description of the photoacoustic spectroscopy setup (b).

[21,23,25]:

$$\mu = \sqrt{\frac{D}{\pi f}} \quad (1)$$

where $\mu$ denotes the thermal diffusion length representing the scanning depth of the spectrometer; $D$ denotes the thermal diffusivity of the leaf, $D \approx 10^{-4}$ cm$^2$ s$^{-1}$ for the polymer materials [21,22]; and $f$ denotes the modulation frequency (Hz), which equals wavenumber multiplied moving mirror velocity.

## 3. Results

### 3.1. Photoacoustic spectra of rice leaves

The photoacoustic spectra of three rice leaf disc samples, one sample from each treatment (N1, N2 and N3), are shown in Fig. 2 (a, b and c, respectively) around 900–4000 cm$^{-1}$ with three moving mirror velocities of 0.32, 0.47, and 0.63 cm s$^{-1}$. It showed that, from the same sample, there were various remarkable absorption peaks had been detected and peaks at the same wavenumber region might with different photoacoustic signal intensity or could not always be detected by different moving mirror velocities. Well-resolved peaks acquired by all the three moving mirror velocities were successfully interpreted to the main functional groups accordingly. The broad bands around 3400 cm$^{-1}$ corresponded to the O—H and N—H stretching vibration. Small shoulder peaks at 2800 cm$^{-1}$ resulted from the C—H stretching vibration. Peaks located at 1650 cm$^{-1}$ overlapped with amide I (C═O) and C═C stretching vibration. In the fingerprint region (900–1200 cm$^{-1}$), the bands occurring at 1050 cm$^{-1}$ were assigned to C—O or Si—O stretching mode. Furthermore, small bands acquired by 0.32 cm s$^{-1}$ (or 0.47 cm s$^{-1}$ sometimes) around 1520 cm$^{-1}$ were relevant to the stretching vibration of aromatic rings and the bending vibration of amide II (N—H). In addition, weak peaks around 2300 cm$^{-1}$ were the nosing signal deprived from $CO_2$ [8,23,26–28].

### 3.2. Diverse variety manners of the spectra from different layer of leaves with three nitrogen treatments

According to Eq. (1), when the thermal diffusivity is stationary, the scanning depth is a function of moving mirror velocity and wavenumber. Thus, photoacoustic spectra with the three moving mirror velocities of 0.32, 0.47, and 0.63 cm s$^{-1}$ indicated the spectra from different layer of the leaf samples. As shown in Fig. 2 (a, b and c), there were obvious differences in the photoacoustic signal intensity from different layers at the region of 3700–2700 cm$^{-1}$, 1800–1300 cm$^{-1}$ and 1300–900 cm$^{-1}$. Interestingly, samples from the three nitrogen treatments (N1, N2 and N3 respectively) showed diverse variety manners.

At the region of 3700–2700 cm$^{-1}$, the intensity of the two peaks at 3400 cm$^{-1}$ and 2800 cm$^{-1}$ with 0.63 cm s$^{-1}$ tended to be the weakest in all the three treatments, while the peaks with 0.32 cm s$^{-1}$ tended to be the strongest, and the peaks with 0.47 cm$^{-1}$ changed irregularly. At the region of 1800–1300 cm$^{-1}$, the bands of 0.63 and 0.32 cm s$^{-1}$ in all treatments showed the same variety manner to the bands at the region of 3700–2700 cm$^{-1}$, but the bands of 0.47 cm$^{-1}$ changed regularly. The bands with 0.47 cm$^{-1}$ were close to the bands with 0.63 cm$^{-1}$ in N1 and N3 invariably, and nearby the bands with 0.32 cm$^{-1}$ in N2 only.

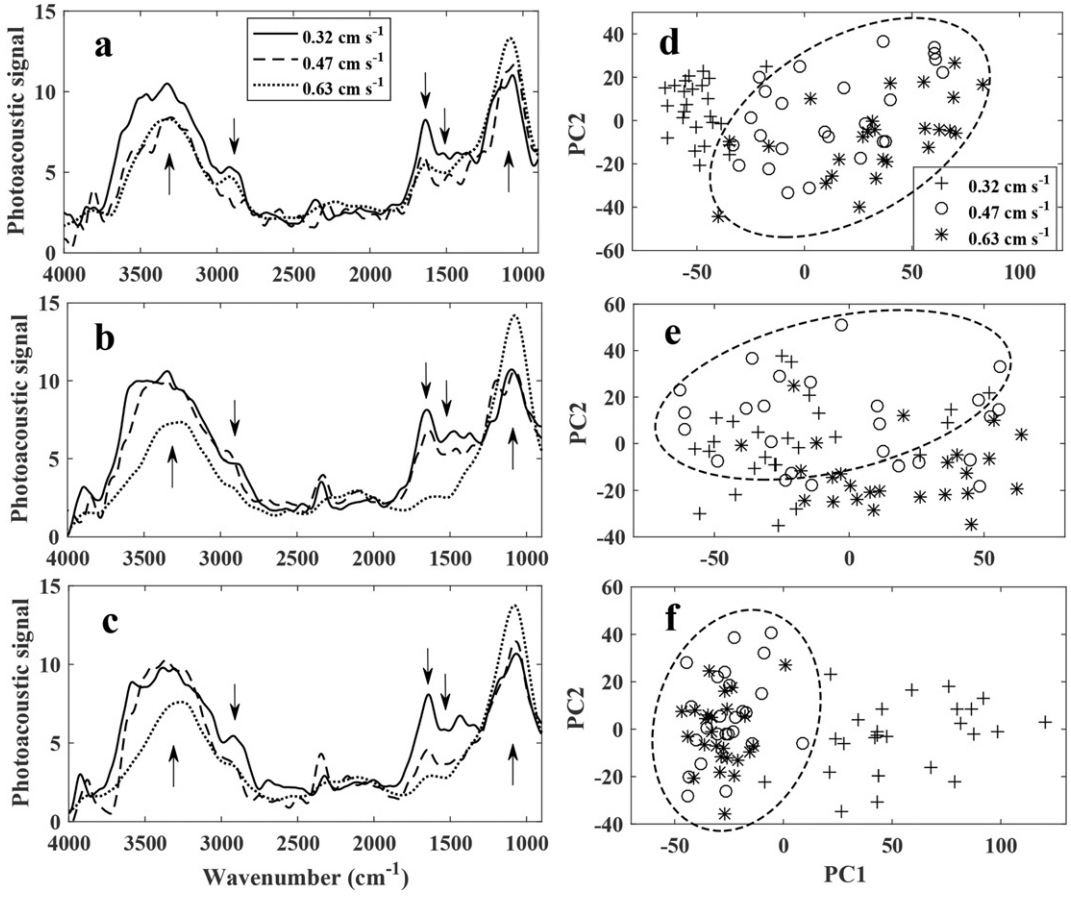


**Fig. 2.** The photoacoustic spectra of one sample of rice leaf front surface (a, b, c) and the principal component (PCA) for all the samples in each set respectively (d, e, f). There were three sets (a, d) (b, e) and (c, f) corresponded to low nitrogen supplies referred as N1, medium nitrogen supplies referred as N2, high nitrogen supplies referred as N3, respectively. The spectra were recorded by three moving mirror velocities of 0.32, 0.47 and 0.63 cm s$^{-1}$ for each set, and the arrows show the typical absorption bands. The first (PC1) and second (PC2) principal components of 75 leaf disc samples in total for each set were used for distributions analysis.

Furthermore, in N1 and N3, the photoacoustic signal intensity of the peaks around 1650 and 1520 $cm^{-1}$ with 0.63 and 0.47 cm $s^{-1}$ were weaker than 0.32 cm $s^{-1}$ and the peak at 1520 $cm^{-1}$ almost disappeared. But in N2, only the peaks with 0.63 cm $s^{-1}$ had the same variety manner. At the region of 1300–900 $cm^{-1}$, the intensity of the peak at 1050 $cm^{-1}$ with 0.63 cm $s^{-1}$ always was the strongest in all the three treatments, and the peaks with 0.32 and 0.47 cm $s^{-1}$ were weaker but without dramatically difference between each other.

It was observed that, with three moving mirror velocities, the spectra appearance was similar or different to each other among some characteristic wavenumber regions. So that it was difficult to directly differentiate the variety manner of the spectra at full spectrum region (900–4000 $cm^{-1}$) in the three nitrogen treatments. Therefore, PCA analysis was conducted, and distributions of principal components (PCs) were made for further expressing the variety manner of the spectra from different layers of the leaves (Fig. 2d, e and f). Totally, 75 spectra in each treatment (N1, N2 and N3), one treatment with 5 leaf discs (Fig. 1) from each of 5 leaf sample reduplications and scanned by 3 moving mirror velocities, were involved in the PCA analysis at full spectrum region, and the explained variances of the first principal component (PC1) and the second principal component (PC2) were used to characterize the spectral information. As shown in Fig. 2 (d, e and f), the spectra with 0.47 cm $s^{-1}$ were closer to the spectra with 0.63 cm $s^{-1}$ in N1 and N3, and turned to nearby the spectra with 0.32 cm $s^{-1}$ in N2, which was same to the variety manner of the bands at 1800–1300 $cm^{-1}$ mentioned above. It indicated that, in the leaf surface, the layer scanned with 0.47 cm $s^{-1}$ was more similar to the layer scanned by 0.63 cm $s^{-1}$ when the samples were treated with low and high nitrogen, and was more similar to the layer scanned by 0.32 cm $s^{-1}$ when the samples were treated with medium nitrogen.

### 3.3. The layer of leaf scanned by the three moving mirror velocities

The plant cell is a circumstance rich of protein, nucleosides and the intermediate substances in their synthetic and metabolic pathways, which contributes to the amide I and amid II absorption peaks at 1650 and 1520 $cm^{-1}$ respectively recorded with 0.32 cm $s^{-1}$ in all the three treatment, and with 0.47 cm $s^{-1}$ in medium nitrogen treatments (N2) (Fig. 2a, b and c). Meanwhile, the cuticle covered the outside of epidermal cell is a thin layer without nitrogen practically (Fig. 3), which leads to the weakness or vanish of amide I and amid II recorded with 0.64 cm $s^{-1}$ in all the three treatment, and with 0.47 cm $s^{-1}$ in low and high nitrogen treatments (N1 and N3). As shown in Fig. 3, it indicated that, in all the three nitrogen treatments, most of the scanning layer with 0.32 cm $s^{-1}$ should go deep into epidermal cell, and the scanning layer with 0.63 cm $s^{-1}$ should stay in cuticle. The regular change of the spectra recorded with 0.47 cm $s^{-1}$ among the three nitrogen supplies demonstrated that when the samples in low and high nitrogen (N1 and N3), the cuticle appeared to be thicker than it in medium nitrogen (N2). In the thicker cuticle leaf, most of the scanning layer with 0.47 cm $s^{-1}$ stayed in cuticle and was close to 0.63 cm $s^{-1}$; and in the thinner cuticle leaf, most of it went deep into epidermal cell and was close to 0.32 cm $s^{-1}$.

### 3.4. The variation of spectra recorded from cuticle

The spectra acquired with 0.63 cm $s^{-1}$ were selected to analyze the variation of cuticle because of its stationary scanning layer in cuticle with all the three treatments. Since there was not visible change among the original spectra from the three different nitrogen treatments, the spectra were divided into several isolated peaks at 3400 $cm^{-1}$, 2800 $cm^{-1}$, 2300 $cm^{-1}$, 1650 $cm^{-1}$, 1050 $cm^{-1}$ through curve-fitting (Fig. 4a). The correlation coefficient ($R^2$) between raw spectrum and fitted spectrum was above 0.86, and the standard errors were less than 0.5. And then it presented some regularities of the ratios of 1050/3400, 1050/2800 and 1650/2800 ($cm^{-1}$), which were achieved with the photoacoustic signal intensity of these fitted peaks.

As shown in Fig. 4b, the intensity ratios of 1050/3400 ($cm^{-1}$) were stable in a narrow range of 1–1.25 at all the positions (P1-P5) on the leaf samples treated with the three nitrogen concentrations (N1, N2 and N3). But, with the same nitrogen treatment, the ratios preferred to be higher in the center position of the leaf, and decreased down successively to both sides. The ratios of 1050/2800 ($cm^{-1}$) were shown in Fig. 4c, which kept on going down from low nitrogen to high nitrogen, with the same manner at the five positions. The ratios of 1650/2800 ($cm^{-1}$) (Fig. 4d) were the highest in medium nitrogen treatment (N2), and decreased down in low and high nitrogen treatments (N1, N3) and all the five positions had the same manner. These variations of the ratios revealed that different nitrogen supplies to rice would affect the substance composition of leaf cuticle.

## 4. Discussion

With high sensitivity and resolution to provide chemical fingerprints for the functional groups present in analyte, Fourier transform infrared photoacoustic spectroscopy (FTIR-PAS) was used for analyzing rapeseed [28], Chinese cabbage [27], Chinese medicinal fungus *Cordyceps sinensis* [21], potato chips [22] and many other plant or biological samples. Otherwise, transmission FTIR and ATR-FTIR, other modes to obtain IR spectrum in mid-infrared region, had been utilized to characterize the isolated leaf or fruit cuticles from different species as well [8,29,30]. According to these researches and other references [26], a band main assignment of plant cuticle and cell in the mid-infrared

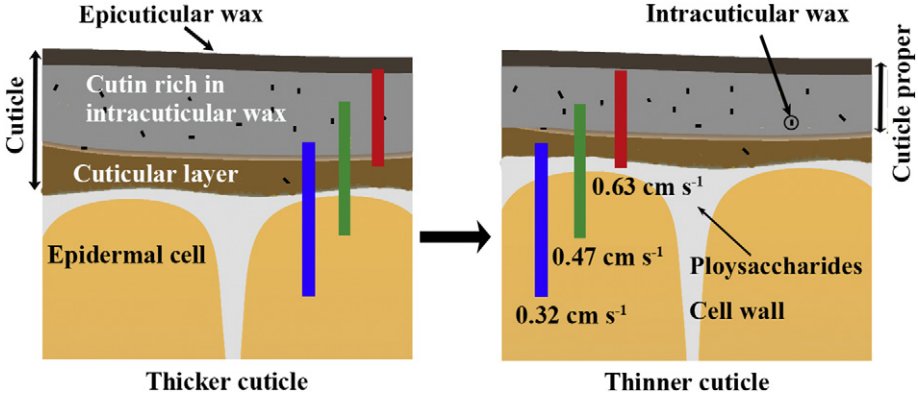


**Fig. 3.** A typical structure of plant cuticle with different thickness on the outer side of epidermal cell. The bands in different colors (blue, green, red) show the scanning layer with of the photoacoustic spectra with different moving mirror velocities (0.32, 0.47, 0.63 cm $s^{-1}$).

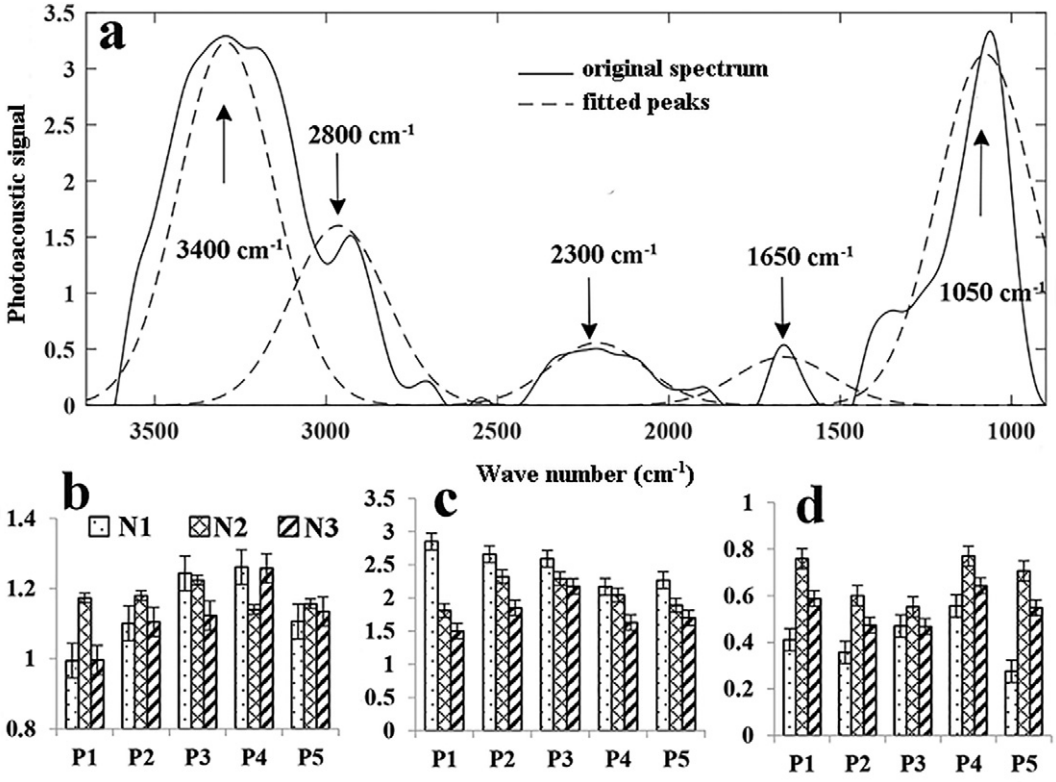


**Fig. 4.** The curve-fitting of one spectrum sample (a) and the variation of the photoacoustic signal intensity ratio between the fitted peaks from all the spectra (b, c, d). (b) 1050/3400, (c) 1050/2800, (d) 1650/2800. N1, N2 and N3 mean low, medium and high nitrogen supplies for each set; P1-P5 means the scanned position selected from leaf samples.

region (900–4000 $cm^{-1}$) is shown in Table 1. Obviously, the assignment was different between plant cell and cuticle.

Plant cuticle proved to be a thin layer about 0.1–10 μm and almost without of nitrogen [3,23]. Notably, in Table 1, the bands associated with N, such as amide I, amide II and N—H stretching vibration at 3400 $cm^{-1}$, usually cannot be detected in cuticle, which was an important evidence for proving the scanning layer of 0.63 cm $s^{-1}$ stayed in cuticle (Fig. 2 and Fig. 3). Furthermore, according to Eq. (1), the profiled depth at the wavenumber region of 900–4000 $cm^{-1}$ with the moving mirror velocity of 0.32 cm $s^{-1}$ was calculated as 1.58–3.33 μm, and it was 1.13–2.35 μm with the moving mirror velocity of 0.63 cm $s^{-1}$. It provided another evidence to reveal that the profiled depth of 0.63 cm $s^{-1}$ may stay in cuticle layer. However, the value of profiled depth could be impacted by the thermal diffusivity (D) of cuticle, which was affected by the heterogeneity and even the wax crystals on the outer face of cuticle. There may be differences between theoretical and practical values.

Rice leaf waxes was reported to contain the major constituents of long-chain alcohols, aldehydes and acids, which accounted for approximately 90% of the total amount of cuticular waxes [9,10]. Both the fatty alcohols and acids would be the source of C—O and O—H, but the C—O stretching vibration from fatty acids emerged around 1200–1300 $cm^{-1}$ [8,22,26], which was different to fatty alcohols at 1050 $cm^{-1}$ (Table 1). In addition, silicon was described to occur in a layer under the wax cuticle [31] or in the crystal-like structures at deeper cuticle areas [2]. There may be the vibrations of Si—O and SiO-H link to the peaks at 1050 and 3400 $cm^{-1}$ respectively as well [2,26]. But considering the amount of fatty alcohols, acids and the cutin composed of hydroxy

**Table 1**
Main attribution for the peaks in mid-infrared region acquired from plant cuticle and cell.

| Wavenumber ($cm^{-1}$) | Vibration[a] | Main attribution | |
|---|---|---|---|
| | | Cell | Cuticle[b] |
| | ν(O—H) | Proteins, nucleosides, aliphatics, saccharides | Fatty alcohols, cutin[c], fatty acid |
| 3400 | ν(N—H) | Proteins, nucleosides | – |
| | ν(C—H) | Proteins, nucleosides, aliphatics, saccharides | Aliphatics[d] |
| 2800 | | | |
| | ν(C=O) | Amide *I* (nucleosides, proteins) | – |
| 1650 | ν(C=C) | Proteins, nucleosides, aliphatics, saccharides | Aliphatics, phenols |
| | δ(N—H) | Amide II (proteins, nucleosides) | – |
| 1520 | ν(aromatic) | Phenolic | Phenols |
| | ν(C—O) | Alcohols, saccharides | Fatty alcohols, cutin |
| 1050 | | | |

[a] The characters ν denotes stretching vibration and δ denotes bending vibration.
[b] The symbol '—' means that the vibration cannot be detected commonly in the cuticle at the specific wavenumber.
[c] Cutin is typically composed of inter-esterified hydroxy fatty acids with embedded polysaccharides.
[d] Aliphatics includes all the aliphatic compounds emerged in cuticle.

fatty acids, the band at 3400 $cm^{-1}$ should be owed to the vibration of $\nu$(O—H) contributed by cutin, fatty acids and alcohols, and the band at 1050 $cm^{-1}$ should be attributed to $\nu$(C—O) in cutin and fatty alcohols, mainly. The stability of the ratio of 1050/3400 ($cm^{-1}$) may due to the high amount of cutin, fatty acids and alcohols (Fig. 4b).

The vibration of $\nu$(C—H) at 2800 $cm^{-1}$ practically exits in all the organic compounds of cuticle (Table 1), which could be used to represent the total amount of cuticle. And the ratio of 1050/2800 ($cm^{-1}$) represents the ratio of $\nu$(C—O)/$\nu$(C—H) reflecting the relative content of the summation of cutin and fatty alcohols, which seems to decrease down with nitrogen concentration increasing up (Fig. 4c).

The bands at 1650 $cm^{-1}$ were assigned to C═C stretching vibration from the unsaturated aliphatics of cuticle mainly (Table 1). Monounsaturated alcohols have been reported in three species of microalgae [32], and in *Arabidopsis thaliana* unsaturated aliphatic components accounted for approximately 60% of the total cutin load [33]. Furthermore, other constituents of cuticle such as phenols and terpenoids may be responsible for the C═C stretching vibration [8,26]. The cutan was thought to be involved in some species cuticle and consist of ether-linked network of methylene chains, double bonds and carboxyl groups and it would result in the absorption at 1650 $cm^{-1}$ as well [2,8]. Hence, the ratio of 1650/2800 $cm^{-1}$ could evaluate the relative content of unsaturated compounds of cuticle (Fig. 4d), which seemed to be high with medium nitrogen, and decreased down with low and high nitrogen.

Although other IR techniques, for instance transmission FTIR and ATR-FTIR, had been taken advantage to analyze cuticle. But the inability for depth-profiling makes them hard to achieve in situ detection, and the cuticles for spectrum recording need to be isolated from plant surface commonly. Through monitoring the modulation frequency, FTIR-PAS can perform depth-profiling, which makes it possible to conduct in situ detection of the cuticle without chemical processes. FTIR-PAS shows a great potential in the in situ and depth-profiling analysis for rice leaf cuticle as well as some other organs and crops.

## 5. Conclusions

The in situ and depth-profiling FTIR-PAS spectra of rice leaf cuticle indicated typical absorption bands, different variation manners were observed in the three nitrogen supplies. Referred to the structure and composition of cuticle, the profiled depth and the potential functional groups contributing to the spectra can be identified. Therefore, in situ and depth-profiling FTIR-PAS provides novel and unique technique to characterize rice leaf cuticle, which shows great potential in detecting how the cuticle response to nitrogen supplies as well as other responses to circumstances for cuticle in other plant.

## Declaration of competing interest

The authors declare that they have no known competing financial interests or personal relationships that could have appeared to influence the work reported in this paper.

## Acknowledgements

The work was financially supported by the National Basic Research Program of China (No. 2015CB150403), the Key Research and Development Project of Jiangsu Province (BE2017388) and the “STS” project from Chinese Academy of Sciences (KFJ-STS-QYZX-046, KFJ-PTXM-003).

## References

[1] A. Heredia, Biophysical and biochemical characteristics of cutin, a plant barrier biopolymer, Biochim. Biophys. Acta Gen. Subj. 1620 (2003) 1–7.
[2] P. Guzmán-Delgado, J. Graça, V. Cabral, L. Gil, V. Fernández, The presence of cutan limits the interpretation of cuticular chemistry and structure: *Ficus elastica* leaf as an example, Physiol. Plant. 157 (2016) 205–220.
[3] G. Vogg, S. Fischer, J. Leide, E. Emmanuel, R. Jetter, A.A. Levy, M. Riederer, Tomato fruit cuticular waxes and their effects on transpiration barrier properties: functional characterization of a mutant deficient in a very-long-chain fatty acid b-ketoacyl-CoA synthase, J. Exp. Bot. 55 (2004) 1401–1410.
[4] C.H. Jeffree, The fine structure of the plant cuticle, in: M. Riedererand, C. Müller (Eds.), Biology of the Plant Cuticle, Blackwell Publishing, Oxford, UK, 2006.
[5] T.H. Yeats, J.K.C. Rose, The formation and function of plant cuticles, Plant Physiol. 163 (2013) 5–20.
[6] D.K. Kosma, M.A. Jenks, Eco-physiological and molecular genetic determinants of plant cuticle function in drought and salt stress tolerance, in: A.J. Matthew, M.H. Paul (Eds.), Advances in Molecular Breeding toward Drought and Salt Tolerant Crops, Springer, Dordrecht, Netherlands, 2007.
[7] E. Domínguez, J.A. Herediaguerrero, A. Heredia, The biophysical design of plant cuticles: an overview, New Phytol. 189 (2011) 938–949.
[8] J.A. Heredia-Guerrero, J.J. Benítez, E. Domínguez, I.S. Bayer, R. Cingolani, A. Athanassiou, Infrared and Raman spectroscopic features of plant cuticles: a review, Front. Recent Dev. Plant Sci. 5 (2014) 305.
[9] K.H. Jung, M.J. Han, D.Y. Lee, Y.S. Lee, L. Schreiber, R. Franke, Wax-deficient anther1 is involved in cuticle and wax production in rice anther walls and is required for pollen development, Plant Cell 18 (2006) 3015–3032.
[10] B. Mao, Z. Cheng, C. Lei, F. Xu, S. Gao, Y. Ren, J. Wang, X. Zhang, J. Wang, F. Wu, X. Guo, X. Liu, C. Wu, H. Wang, J. Wan, Wax crystal-sparse leaf2, a rice homologue of wax2/gl1, is involved in synthesis of leaf cuticular wax, Planta 235 (2012) 39–52.
[11] M. Riederer, L. Schreiber, Protecting against water loss: analysis of the barrier properties of plant cuticles, J. Exp. Bot. 52 (2001) 2023–2032.
[12] K. Koch, W. Barthlott, Superhydrophobic and superhydrophilic plant surfaces: an inspiration for biomimetic materials, Phil. Trans. R. Soc. A 367 (2009) 1487–1509.
[13] V. Fernández, T. Eichert, V.D. Río, G. López-casado, J.A. Heredia-guerrero, A. Abadía, Leaf structural changes associated with iron deficiency chlorosis in field-grown pear and peach: physiological implications, Plant & Soil 311 (2008) 161–172.
[14] D. Cozzolino, Use of infrared spectroscopy for in-field measurement and phenotyping of plant properties: instrumentation, data analysis, and examples, Appl. Spectrosc. Rev. 49 (2014) 564–584.
[15] C. Popa, Ethylene measurements from sweet fruits flowers using photoacoustic spectroscopy, Molecules 24 (2019) 1144.
[16] A. Rosencwaig, A. Gersho, Theory of the photoacoustic effect with solids, J. Appl. Phys. 47 (1976) 64–69.
[17] D.H. Mcqueen, R. Wilson, A. Kinnunen, Near and mid infrared photoacoustic analysis of principal components of food stuffs, Trends Anal. Chem. 14 (1995) 482–492.
[18] R.A.V. Rossel, A.B. McBratney, Soil chemical analytical accuracy and costs: implications from precision agriculture, Aust. J. Exp. Agric. 38 (1998) 765–775.
[19] C. Du, J. Zhou, H. Wang, X. Chen, A. Zhu, J. Zhang, Determination of soil properties using Fourier transform mid-infrared photoacoustic spectroscopy, Vib. Spectrosc. 49 (2009) 32–37.
[20] S. Armenta, J. Moros, S. Garrigues, M.D.L. Guardia, Direct determination of mancozeb by photoacoustic spectrometry, Anal. Chim. Acta 567 (2006) 255–261.
[21] C. Du, J. Zhou, J. Liu, Identification of Chinese medicinal fungus *Cordyceps sinensis* by depth-profiling mid-infrared photoacoustic spectroscopy, Spectroc. Acta. Pt. A-Molec. Biomolec. Spectr. 173 (2017) 489–494.
[22] S. Sivakesava, J. Irudayaraj, Analysis of potato chips using FTIR photoacoustic spectroscopy, J. Sci. Food Agric. 80 (2000) 1805–1810.
[23] G. Lv, C. Du, F. Ma, Y. Shen, J. Zhou, Rapid and nondestructive detection of pesticide residues by depth-profiling Fourier transform infrared photoacoustic spectroscopy, ACS Omega 3 (2018) 3548–3553.
[24] S. Yoshida, D.A. Forno, J.K. Cock, K.A. Gomez, Laboratory Manual for Physiological Studies of Rice, International Rice Research Institute, Manila, Philippines, 1976.
[25] W.R. Zhang, C. Lowe, R. Smith, Depth-profiling of coil coating using step-scan photoacoustic FTIR, Prog. Org. Coat. 65 (2009) 469–476.
[26] R.M. Silverstein, F.X. Webster, D.J. Kiemle, Spectrometric Identification of Organic Compounds, 7th Ed John Wiley & Sons. Inc, Hoboken, USA, 2005.
[27] C. Li, C. Du, Y. Zeng, F. Ma, Y. Shen, Z. Xing, J. Zhou, Two-dimensional visualization of nitrogen distribution in leaves of Chinese cabbage (*Brassica rapachinensis*) by the Fourier transform infrared photoacoustic spectroscopy technique, J. Agric. Food Chem. 64 (2016) 7696–7701.
[28] Y. Lu, C. Du, C. Yu, J. Zhou, Use of FTIR-PAS combined with chemometrics to quantify nutritional information in rapeseeds (*Brassica napus*), J. Plant Nutr. Soil Sci. 177 (2014) 927–933.
[29] F.J. Ramírez, P. Luque, A. Heredia, M.J. Bukovac, Fourier transform IR of enzymatically isolated tomato fruit cuticular membrane, Biopolymers 32 (1992) 1425–1429.
[30] L. España, J.A. Heredia-Guerrero, P. Segado, J.J. Benítez, A. Heredia, E. Domínguez, Biomechanical properties of the tomato (*Solanum lycopersicum*) fruit cuticle during development are modulated by changes in the relative amounts of its components, New Phytol. 202 (2014) 790–802.
[31] P. Bauer, R. Elbaum, I.M. Weiss, Calcium and silicon mineralization in land plants: transport, structure and function, Plant Sci. 180 (2011) 746–756.
[32] J.K. Volkman, S.M. Barrett, S.I. Blackburn, Eustigmatophyte microalgae are potential sources of C29 sterols, C22-C28 n-alcohols and C28-C32 n-alkyl diols in freshwater environments, Org. Geochem. 30 (1999) 307–318.
[33] G. Bonaventure, F. Beisson, J. Ohlrogge, M. Pollard, Analysis of the aliphatic monomer composition of polyesters associated with Arabidopsis epidermis: occurrence of octadeca-cis-6, cis-9-diene-1, 18-dioate as the major component, Plant J. 40 (2004) 920–930.